Robert J. Steighner,[1] Ph.D.; Lois A. Tully,[2] Ph.D.; Justin D. Karjala,[1] M.F.S.; Mike D. Coble,[1] M.F.S.; and Mitchell M. Holland,[1] Ph.D.

Comparative Identity and Homogeneity Testing of the mtDNA HV1 Region Using Denaturing Gradient Gel Electrophoresis*

REFERENCE: Steighner RJ, Tully LA, Karjala JD, Coble MD, Holland MM. Comparative identity and homogeneity testing of the mtDNA HV1 region using denaturing gradient gel electrophoresis. J Forensic Sci 1999;44(6):1186–1198.

ABSTRACT: A denaturing gradient gel electrophoresis (DGGE) assay has been developed for comparative identity and homogeneity testing of the mtDNA HV1 region. A total of 49 pairs of sequences, each pair differing by a single unique polymorphism, were tested to verify the reliability of the assay. Discrimination between all pairings was achieved as judged by the resolution of the mismatch-containing heteroduplexes from the fully base-paired homoduplexes. In all but two pairings, resolution of the fully base-paired homoduplexes was also obtained. Sequence pairs differing by multiple polymorphisms were also tested and resulted in a greater separation between the homo- and heteroduplexes. Additional information derived from the technique includes the identification of co-amplifying contaminating or heteroplasmic samples in the independent samples lanes. Thirteen heteroplasmic samples, six at positions distinct from those analyzed in the pairwise comparison study, were analyzed and the heteroplasmic positions identified unambiguously by sequencing the excised bands. The technique constitutes a conceptually simple, accurate, and inexpensive test for determining whether two sequences match within the mtDNA HV1 region, while providing a more definitive control for the identification of co-amplifying contaminating or heteroplasmic sequences than is presently available.

KEYWORDS: forensic science, DNA typing, mitochondrial DNA, denaturing gradient gel electrophoresis, heteroduplex, sequence matching, human identification

Mitochondrial DNA sequence analysis is utilized in a number of fields including forensic science (1–6), population and evolutionary biology (7–9), and anthropology (10). The discriminatory power of the technique arises from the polymorphic characteristics of the hypervariable regions 1 and 2 located within the mitochondrial displacement loop (D-loop) (11–16). Typing of samples is made by comparing the polymorphisms found in HV1 and HV2 with those of a matrilineal reference in forensics, or from a known population databases in evolutionary biology or anthropology. Barring mutation, maternally related sequences will be identical due to the haploid inheritance of mitochondria (17). The current forensic procedure requires the amplification and sequencing of both the HV1 and HV2 regions from the sample and a reference standard before any comparison may be made (5,18–21). If the sequences are different, an exclusion may be made while identical sequences are used to support a match. Regardless of the outcome, the current sequencing procedure requires a considerable commitment in time and money before any decision regarding a match is made. Comparing two PCR products by DGGE has the potential to expedite the overall process by excluding non-matches without having to sequence the samples. An additional benefit is the unambiguous identification of heteroplasmic or co-amplifying contaminating sequences at levels of sensitivity generally unobtainable through conventional sequencing.

Denaturing gradient gel electrophoresis (DGGE) (22–28), temperature gradient gel electrophoresis (29–31), and the constant denaturant derivatives of those procedures including constant denaturing gel electrophoresis (32–34) and more recently constant denaturing and temperature-programmed capillary electrophoresis (35,36) are all capable of resolving DNA sequences differing by a single polymorphism. The techniques exploit the sensitivity of specified regions of DNA, defined by sequence, to denature under specific temperature or chemical denaturant concentrations. As the temperature or concentration of chemical denaturants is raised, DNA dissociates in a discontinuous but predictable manner indicative of the melting of unique domains. In DGGE, DNA migrates through an acrylamide gel of increasing chemical denaturant until reaching the point where the denaturant concentration is equivalent to the melting temperature of the lowest melting domain within the fragment. At this point, strand dissociation occurs retarding further migration. Differential base-stacking energies between polymorphisms in an otherwise identical fragment impart small, but exploitable differences in the stability of the domain in which they reside. Those differences are sufficient to result in an unambiguous separation between two sequences on acrylamide gels. Most single base pair polymorphisms between two fully base-paired fragments differ in stability enough to be resolved from one another by the technique. However, the probability of resolving two dissimilar sequences is enhanced by "heteroduplexing," or mixing, heat denaturing, and allowing the two sequences to reanneal. If the two sequences are identical, only a single species will be present in the

[1] Armed Forces DNA Identification Laboratory, Office of the Armed Forces Medical Examiner, The Armed Forces Institute of Pathology, 1413 Research Boulevard, Rockville, MD.

[2] University of Maryland at Baltimore, School of Medicine, Division of Human Genetics, Baltimore, MD.

* The opinions and assertions expressed herein are solely those of the author and are not to be construed as official or as the views of the United States Department of Defense or the United States Department of the Army. This work was supported by a grant from the American Registry of Pathology and intramural funds from the Armed Forces Institute of Pathology.

Received 20 Oct. 1998; and in revised form 11 Feb. 1999; accepted 15 Feb. 1999.

sample upon renaturation. If different, the sample will contain both the original fully base-paired homoduplexes and a pair of hybrid-heteroduplexes, composed of a single strand from each of the original homoduplexes but having a mismatch at the site of each polymorphism. Mismatch containing sequences are readily resolved by DGGE since they have large effects on the stability of the melting domains in which they reside (37,38). In forensic testing, a match between two samples may be obtained by heteroduplexing the reference and test sample (Fig. 1). Identical sequences would yield a single matching band in both the mixed and independent sample lanes. Conversely, multiple bands in the mixed sample lane would indicate dissimilar sequences excluding a match, while heteroplasmy or co-amplifying contaminating sequences would be revealed by multiple bands in the independent sample lane.

Methods and Materials

PCR products used in this study were designed to be compatible with those products generated in mitochondrial casework in our laboratory. Since PCR amplification of degraded DNA samples is more successful when smaller regions are amplified (39,40), the standard PCR reaction for the HV1 region in our laboratory amplifies the region in two sections. Primer set 1 (PS1) is designed to amplify the proximal portion (bp 16024 to 16235) of HV1, and primer set 2 (PS2) the distal region (bp 16165 to 16365) (5). The HV1 region proved quite amenable to DGGE in that the same primers used in casework could be modified by attaching a GC-clamp to the primer and used directly for DGGE analysis. Of the two hypervariable regions in the mitochondrial D-loop, the HV1 region is more polymorphic, and therefore the most useful in terms of discrimination potential (41). Primer sets PS1A (L15989GC/H16258; 310 bp) and PS1B (L15989/H16258GC; 310 bp), which differ only by placement of the GC-clamp, and PS1C (L16014/H16258GC; 285 bp), were all used for the 5′ end of HV1. The use of PS1C was discontinued because it does not include the first ten bases of HV1. Primer set PS2 (L16144GC/H16410; 306 bp) amplified the 3′ end of HV1. Amplification with either PS1A or PS1B, along with PS2 is sufficient to analyze the entire HV1 region (bp 16024-16365). Primer sequences can be found in Table 1.

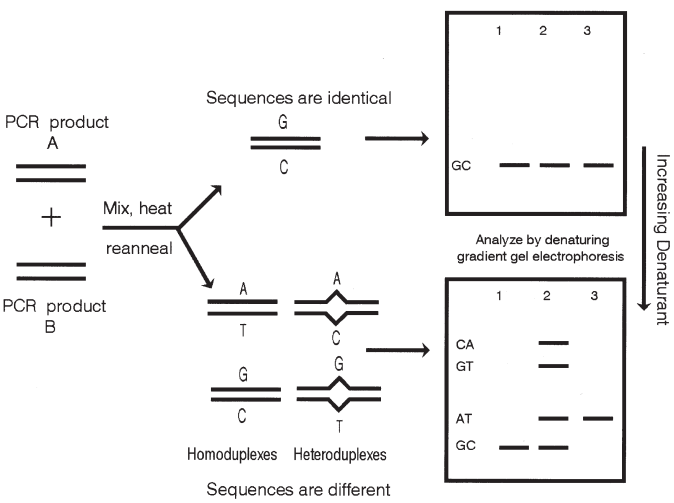

FIG. 1—*Schematic outline of procedure in which two PCR products (A + B) are mixed, heated, and allowed to reanneal. If the sequences are identical a single band will appear on the denaturing gradient gel in both the mixed and independent sample lanes. If different, multiple bands will appear in the mixed sample lane. Lanes one and three are the independent samples lanes and lane two is the mixed sample lane.*

PCR

Total cellular DNA was prepared from whole blood samples using either the Purgene DNA isolation kit (Gentra, Minneapolis, MN), the QIAamp blood extraction kit (Qiagen, Santa Clarita, CA) according to manufacturers instructions, or by chelex extraction from blood cards as previously described (42). Samples were amplified with either *pfu* polymerase (Stratagene, La Jolla, CA), *AmpliTaq* polymerase or *AmpliTaq* Gold polymerase (Perkin-Elmer Inc., Foster City, CA). The standard 50 μL PCR reaction for *pfu* polymerase reaction contained 1X *pfu* buffer (200 mM Tris-HCL (pH 8.75), 100 mM KCL, 100 mM $(NH_4)_2SO_4$, 20mM $MgSO_4$, 1% Triton® X-100, 1 mg/mL bovine serum albumin), 0.2 μM primers, 0.2 mM dNTPs (Life Technologies, Germantown, MD), and 2.5 units of *pfu* polymerase. The standard *AmpliTaq* reaction contained 1X *AmpliTaq* buffer (10 mM Tris-HCl (pH 8.3), 50 mM KCl, and 1.5 mM $MgCl_2$), 0.2 μM primers, 0.2 mM dNTPs, and 2.5 units of *AmpliTaq* polymerase. Amplifications with *AmpliTaq* Gold were identical except for a ten-minute heat activation step at 94°C prior to cycling. Amplification parameters for the PS2 reactions were denaturation at 95°C for 15 s, annealing at 60°C for 10 s, and extension at 72°C for 20 s. Thirty-five PCR cycles were run for PS2. Identical reaction conditions were employed for the PS1B and PS1C reactions. Amplification with the PS1A primer set often resulted in higher background (see Fig. 4A) on the gels not seen with PS1B. A 62.5°C annealing temperature (forty cycles) was employed for those reactions with limited success in reducing that background. The problem could interfere with identifying low level heteroplasmy in lanes with significant background. PCR reactions were performed in a GeneAmp® 9600 thermal cycler (Perkin-Elmer, Foster City, CA). All 20-mer primers (Table 1) were synthesized on a Perkin-Elmer DNA synthesizer model 394. The 60-mer, GC-clamped primers, were purchased HPLC or acry-

TABLE 1—*Sequences of PCR primers used in experiments. Numbering (5′→3′ direction) is consistent with Anderson et al. (43), but does not include the GC-clamp (underlined) portion of the primer.*

L15989 – CCCAAAGCTAAGATTCTAAT
L16014 – CTATTCTCTGTTCTTTCATGGG
L16144 – TGACCACCTGTAGTACATAA
H16410 – GAGGATGGTGGTCAAGGGA
H16258 – TGGCTTTGGAGTTGCAGTTG
H16258GC – CGCCCGCCGCGCCCCGCGCCCGTCCCGCCGCCCCCGCCCGTGGCTTTGGAGTTGCAGTTG
L15989GC – CGCCCGCCGCGCCCCGCGCCCGTCCCGCCGCCCCCGCCCGCCCAAAGCTAAGATTCTAAT
L16144GC – CGCCCGCCGCGCCCCGCGCCCGTCCCGCCGCCCCCGCCCGTGACCACCTGTAGTACATAA

lamide gel purified from Biosynthesis Inc. (Lewisville, TX) or Synthetic Genetics (San Diego, CA). GC-clamps were used to transform the melting characteristics of the attached targeted mitochondrial region and to impart a high melting domain into the final PCR product (38,44–66). Primers were quantitated by ultraviolet absorbance at 260 nm and diluted in TE (20 mM Tris-EDTA) or dH_2O. Success of the PCR reactions was determined by electrophoresis of a 5 μL aliquot of the product with 1–2 μL of loading buffer (50% glycerol, 1.5 mM bromophenol blue, and 100 mM EDTA) and analyzed on 1–2% agarose gels (Life Technologies) or 3% Nusieve (3:1) gels (FMC, Rockland, ME). Size and concentration of PCR products were estimated by electrophoresis with molecular weight concentration standards. Agarose gel electrophoresis was performed at 90–100 V for 1–2 h in 1X TBE (89 mM Tris-HCL, 89 mM boric acid, 2 mM Na_2EDTA, pH 8.3) containing 0.5 μg/mL ethidium bromide.

Denaturing Gradient Gel Electrophoresis

Parallel denaturing gradient gels (22 cm × 17.7 cm × 1 mm) were electrophoresed for 16–18 h at 3–4.5 V/cm submerged in a 30 L tank (lower buffer chamber) designed for DGGE (C.B.S. Scientific, Del Mar, CA). Buffer (40 mM Tris-acetate and 10 mM EDTA) was circulated continuously between upper and lower buffer chambers with a peristaltic pump, and maintained at a constant temperature of 60°C. The denaturant gradient concentration for parallel gels was between 40 and 50% denaturant for the PS1B, PS1C, and PS2 products and 37.5 and 47.5% for the PS1A products (100% denaturant was defined as 7 molar urea and 40% formamide). Gradient used for mobility transition gels (perpendicular denaturing gradient gels) was 0 and 80%. The gradients were poured with a manual gradient maker using gravity flow. Final acrylamide concentration was 6.5% acrylamide:bis-acrylamide (37.5:1) unless stated otherwise. Polymerization of gels was initiated by addition of 0.1% ammonium persulfate and 0.01% TEMED (N,N,N′,N′-tetramethylethylenediamine).

The narrow gradients used in this study are equivalent to only a 3.1°C temperature change between the top and bottom of the gel (26). This range was chosen to maximize resolution of the homoduplexes, however, precise and consistent pouring of the gradient is critical. Sides of gel cassettes were taped with electrical tape and the outer two lanes on the gels were generally not used due to the electrical interference from the surrounding lower buffer chamber. Perpendicular denaturing gradient gels were poured as described above, with the exception that 0.04% TEMED was employed to expedite polymerization and the samples were loaded in a single well extending across the top of the gel. Perpendicular gels were run for 6 h at 4.5 V/cm. Each PCR product pair to be tested was mixed, heat denatured (10 min at 99°C), and allowed to reanneal by slowly cooling to room temperature for at least 15 min. Each independent sample was also heated to 99°C for 10 min and allowed to cool to room temperature in parallel. After reannealing, 2 μL of loading buffer (50% glycerol, 1.5 mM bromophenol blue, and 100 mM EDTA) was added and the sample loaded onto denaturing gradient gels. Between 0.1 and 1 μg of PCR product was loaded per well. Gels were stained with Sybergreen I (20 μg/mL) for 30–60 min following electrophoresis. The relative proportion of each band in heteroplasmic samples was determined by integrating peak intensities from the scanned gel image on a Power Macintosh computer using the public domain NIH image program (developed at the U.S. National Institutes of Health and available on the Internet at http://rsb.info.nih.gov/nih-image/).

Sequencing

Both the homo- and heteroduplex bands found in samples suspected of being heteroplasmic were excised from the gels, crushed with a spatula, and incubated in 100 μL dH_20 for 16–18 h (overnight) at 56°C in a microfuge tube. Samples were centrifuged for 10 min at 5000 g to sediment the larger pieces of acrylamide and an aliquot was re-amplified as above for 35 cycles using non-GC-clamped primers (L15989 and H16258 for PS1A or PS1B, L16014 and H16258 for PS1C and L16144 and H16410 for PS2). The resultant PCR products were sequenced in a GeneAmp® 9600 thermal cycler using the Prism Ready Dye Terminator Cycle Sequencing Kit with *AmpliTaq* DNA polymerase, FS (Taq, FS; Perkin-Elmer/Applied Biosystems Division, Foster City. CA.) according to manufacturer's instructions. Excess dye-terminators were removed by spin-column centrifugation using AGTC cartridges (Advanced Genetic Technologies Corp., Gaithersburg, MD), and evaporated to dryness. Samples were re-suspended in 4 μL of loading buffer (5:1 deionized formamide: 50 mM EDTA) and analyzed on an Applied Biosystems 373A Sequencer.

Results

Mobility Transition Gels (Perpendicular Denaturing Gradient Gels)

The melting profiles (Fig. 2A,C,E) of the native mitochondrial HV1 sequence and the PCR products used in the experiments were determined using the computer programs Poland (47) and Melt87 (26). Each figure depicts the temperature at which each base pair in the sequence is in 50/50 equilibrium between a fully base-paired or non-base-paired, dissociated, configuration. Computer analysis of the region predicted that attaching GC-clamps to either of the complementary primers for PS1 (PS1A and PS1B) as well as to primer F16144 for PS2, would produce two fragments in which all heteroduplexes within the HV1 region may be expected to be resolved from their respective homoduplexes. Together, the two primer sets provide redundancy in the overlapping region (bp 16164 to 16238). Experimental verification of the computer-generated melt maps was obtained by running mobility transition gels (Fig. 2B,D,F). Each fragment was electrophoresed through a 0 to 80% denaturant gradient running perpendicular to the direction of migration. Denaturation of distinct melting domains was reflected by a decrease in migration rate and retardation of the fragment in the gel. A single sigmoidal transition was obtained for each individual melting domain (except the highest melting domain) contained within a given fragment. Confirmation of the melt maps was obtained for each of the primer sets used in the analysis of the HV1 region. This region contains a more stable domain located in the middle (light line in Fig. 2A,C,E) which is reflected in the higher stability of the intermediate domain of fragment PS1B and in the 5′ end of the PS2 fragment (see legend Fig. 2).

Analysis of Single-Base Pair Differences on Parallel Denaturing Gradient Gels

In all comparisons, fragments containing a mismatch were easily resolved from their respective fully base paired homoduplexes (Table 2 and Figs. 3 and 4). This alone is enough to exclude a match between two sequences. However, analysis of the data generated with the two PS1 primer sets revealed profound differences in the resolution of the fully base-paired homoduplexes, four of which are shown in Fig. 5. The positions affected were all located toward the

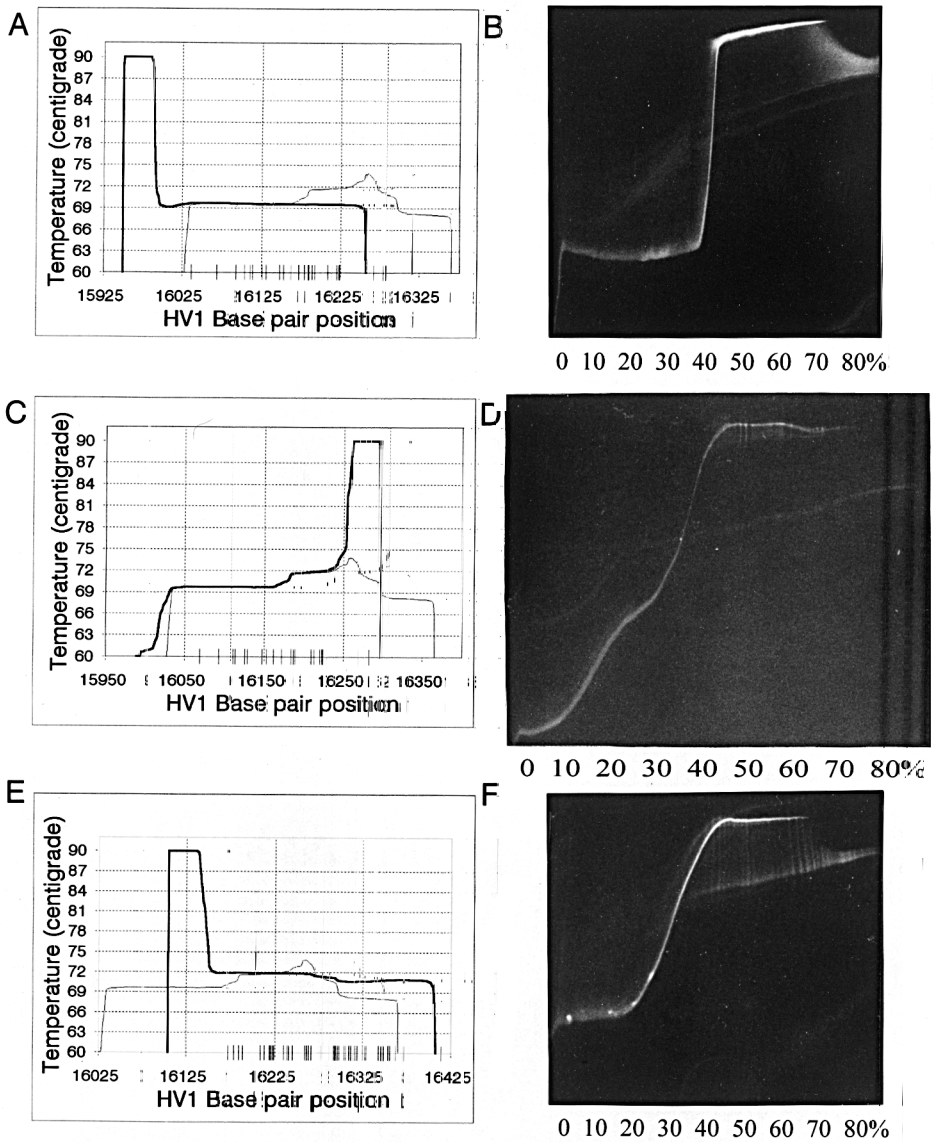

FIG. 2—*Computer generated melt maps (Fig. 2A,C,E) and mobility transition gels (Fig. 2B,D,F) of the PCR products amplified in this study. The temperature (T_m) at which each nucleotide in the sequence is expected to be in 50/50 equilibrium between base paired and non-base paired configurations are plotted versus sequence position. Melting characteristics of the consensus standard sequence (43) between bp 16024 and 16365 are also depicted in each of the figures (thin line). The position of each polymorphism analyzed in relation to the melting map for each fragment is shown as tick marks on the abscissa in the meltmaps. Approximate percent denaturant is shown on the abscissa for each of the mobility transition curves. Figure 2A depicts the PS1A fragment which contains two separate melting domains, a high melting domain ($T_m \approx 90°C$) on the 5′ end imposed by the GC-clamped primer and a lower melting domain ($T_m \approx 70°C$) encompassing the rest of the fragment. Confirmation of the melt map is shown in the mobility transition gel (Fig. 2B) which depicts a single sharp sigmoidal transition curve consistent with the presence of a single domain encompassing the targeted region. Figure 2C depicts the melt map for the PS1B fragment containing three distinct domains. In addition to the high melting domain imposed by the GC-clamp, the fragment contains an intermediate melting domain (bp 16175 to 16230) with a $T_m \approx 72°C$, and a low melting domain (bp 16025 to 16175) with a $T_m \approx 70°C$. The mobility transition gel for the fragment (Fig. 2D) displays two separate sigmoidal transitions, one for each of the lower melting domains. Decreased migration commensurate with dissociation of the lowest melting domain precludes resolution of the more stable homoduplexes in this region (see Fig. 5). Melt map of the PS1C fragment used in the Romanov case was essentially identical to that of PS1B. Figure 2E and F depict the PS2 fragment which, in addition to the high melting domain contributed by the GC-clamp, apparently reveal a single domain encompassing the region of interest but one in which the transition is considerably less steep than that found with the PS1A fragment. In fact, the region does not contain a single uniform domain but is somewhat heterogeneous with respect to T_m, with the 5′ end of the targeted region (bp 16163-16300) displaying a slightly higher T_m then the 3′ end. Although subtle, the shallower slope seen in the mobility transition gel (Fig. 2F) is indicative of the non-homogeneous denaturation behavior of the region believed responsible for the lack of separation seen with the more stable homoduplexes in the parallel denaturing gels. The 5′ ends of PS1A and PS2, and the 3′ end of PS1B are composed of GC-clamp sequence and not the corresponding mitochondrial sequence as depicted in the figure.*

TABLE 2—*Distribution (Table 2A) of single base polymorphic differences analyzed in the pairwise comparison study (bold) or heteroplasmic samples (bold and underlined) identified within the mtDNA HV1 region (16024 to 16365). Sample pairing, position, polymorphism, and fragments analyzed are listed in Table 2B. Twenty-eight out of 64 possible three base triplets were analyzed in this study. CRS stands for the Cambridge reference sequence (43).*

2A

16024 – TTCTTTCATGGGG**A**AGCAGATTTGGGTACCACCCAAGTATTGACT**C**ACCCAT
16076 – CAACAACCGCTATGTAT**T**TCGTACATTA**C**TGCCAG**C**CA**C**CATGAATATTG**T**A
16128 – C**G**GT**T**ACCATAAATACTTGAC**C**ACCT**G**TAGTACAT**A**AAAACC**C**AA**T**CCACAT**C**
16180 – AAAA**C**C**C**CCC**T**CC**C**CATGCTTACAAGCAAG**T**ACA**G**CAATC**AA**CC**CT**CAACTAT
16232 – CAC**A**CAT**C**AACTG**C**AACTCCAAAGCCA**C**C**C**C**T**CA**C**CCACTAGGATA**C**CAACA
16284 – AAC**C**TAC**CCACCC**TT**T**AA**C**AG**T**ACAT**A**G**T**ACATA**A**A**AG**CCATT**T**A**C**CGTACATA
16336 – GCACATT**A**CAGTCAAATC**C**C**T**TCTCG**T**CCC

2B	Sample (s)	MtDNA Position	Polymorphism and Nearest Neighboring Nucleotides	Product Analyzed*
1	B10/B11	16037	GAA>GGA	1
2	E114/E111	16069	TCA>TTA	1,3
3	M7/CRS‡	16093	TTT>TCT	1,2,3
4	B17/B23	16104	ACT>ATT	1
5	E47/CRS	16111	GCC>GTC	1
6	J4/J2	16114	ACC>ATC	1,2,3
7	E117/CRS‡	16126	GTA>GCA	1,2,3
8	E74/CRS‡	16129	CGG>CAG	1,2,3
9	B18/CRS	16131	GTA>GCA	1
10	E96/E66	16148	CCA>CTA	1,2,3
11	B15/CRS†	16153	TGT>TCT	1
12	E29/E75	16162	TAA>TGA	1,2,3
13	Romanov's‡	16169	CCA>CTA	3
14	E12/E86‡	16172	ATC>ACC	1,2,3,4
15	M1/CRS	16179	TCA>TTA	1,2
16	E53/E99	16184	ACC>ATC	1,2,3,4
17	M6‡	16185	CCC>CTC	1
18	E119/CRS	16189	CTC>CCC	1
19	B12/CRS‡	16192	CCC>CTC	1,2,3,4
20	E44/CRS	16209	GTA>GCA	1,2,4
21	E73/CRS	16213	AGC>AAC	1,2,4
22	B2/B1	16219	CAA>AGC	4
23	N3/CRS†	16220	AAC>ATC	1,2,4
24	B8/CRS	16221	ACC>ATC	4
25	E100/CRS	16223	CCT>CTT	1,2,3,4
26	E109/E105	16224	CTC>CCC	1,2,3,4
27	B9/CRS	16235	CAC>CGC	4
28	E93/CRS†	16239	TCA>TGA	4
29	B7/B11	16245	GCA>GTA	4
30	M5/E105	16259	ACC>ATC	4
31	B6/CRS	16261	CCC>CTC	4
32	M4/E105	16263	CTC>CCC	4
33	E115/E105	16266	ACC>ATC	4
34	E80/CRS	16278	ACC>ATC	4
35	P1‡	16287	CCT>CTT	4
36	B13/CRS†	16291	CCC>CGC	4
37	E4/CRS	16292	CCA>CTA	4
38	B5/CRS	16293	CAC>CGC	4
39	M3/CRS	16294	ACC>ATC	4
40	B24‡	16295	CCC>CTC	4
41	M3/E117	16296	CCT>CTT	4
42	N1/CRS	16298	TTA>TCA	4
43	M8‡	16301	ACA>ATA	4
44	E20/CRS	16304	GTA>GCA	4
45	B4/CRS‡	16309	TAG>TGG	4
46	E5/CRS‡	16311	GTA>GCA	4
47	E74/E97	16316	TAA>TGA	4
48	R1†‡	16318	AAG>ATG	4
49	B3/CRS	16319	AGC>AAC	4
50	B25/CRS	16325	TTA>TCA	4
51	E51/CRS	16327	ACC>ATC	4
52	E120/CRS	16343	TAC>TGC	4
53	M2/CRS	16354	CCC>CTC	4
54	N2/E19	16356	CTT>CCT	4
55	E19/CRS	16362	GTC>GCC	4

* Primer sets used in the analysis include: (1) PS1A; (2) PS1B; (3) PS1C; (4) PS2.
† Indicates a transversion.
‡ Positions at which heteroplasmy was found.

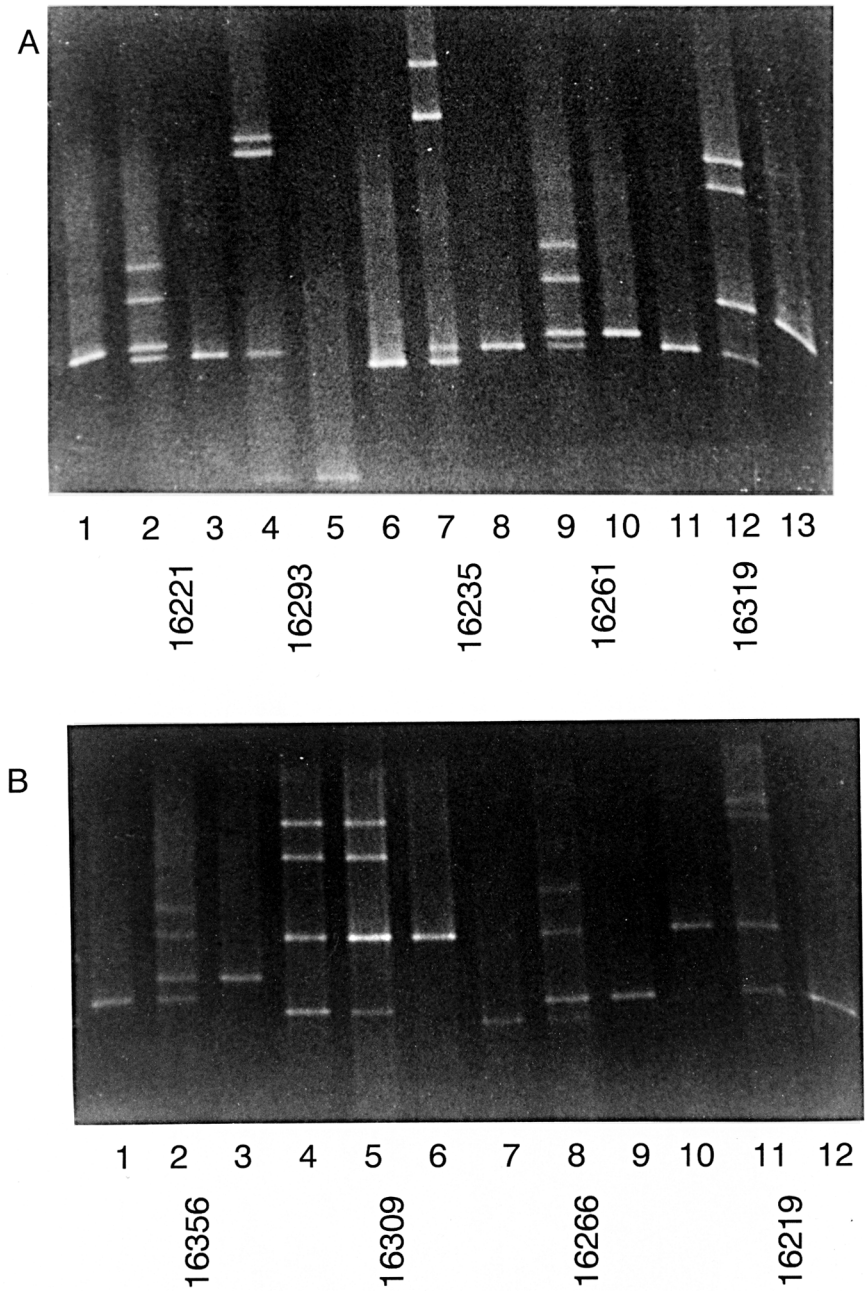

FIG. 3—*40 to 50% parallel denaturing gradient gels of the PS2 fragment with each comparison differing by a single base pair at the indicated positions (polymorphisms are listed in Table 2). Each mixed sample pair is flanked by the individual samples in the adjacent lanes. In the mixed sample lanes the two lower bands represent the more stable, fully base paired homoduplexes and the upper bands the mismatch containing heteroduplexes. Sample B4 (lane 4, Fig. 3B) is heteroplasmic at position 16309 (A+G) with the two sequences present at equivalent concentrations. Lane assignments for each gel are as follows:* Figure 3A: *Lane 1, B8; Lane 2, B8/CRS; Lane 3, CRS; Lane 4, B5/CRS; Lane 5, B5 (homoduplex band for sample B5 is very light and located toward the bottom of the figure in both lanes 4 and 5); Lane 6, B9; Lane 7, B9/CRS; Lane 8, CRS; Lane 9, B6/CRS; Lane 10, B6; Lane 11, CRS; Lane 12, B3/CRS; Lane 13, B3.* Figure 3B: *Lane 1, N2; Lane 2, N2/E19; Lane 3, E19; Lane 4, B4 Lane 5, B4/CRS; Lane 6, CRS; Lane 7, E105; Lane 8, E105/E115; Lane 9, E115; Lane 10, B2; Lane 11, B2/B1; Lane 12, B1.*

A

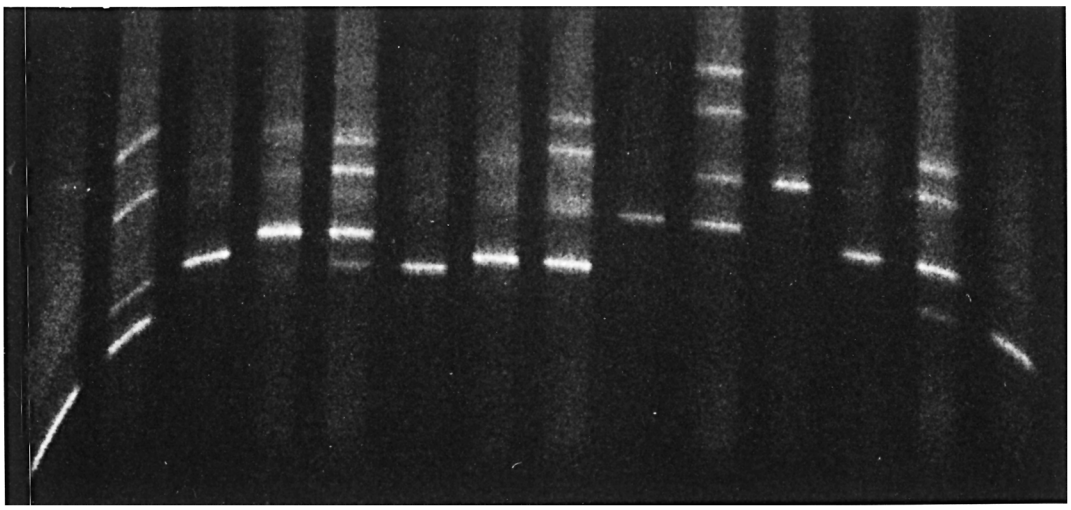

1 2 3 4 5 6 7 8 9 10 11 12 13 14

16184 16037 16153 16126 16069

B

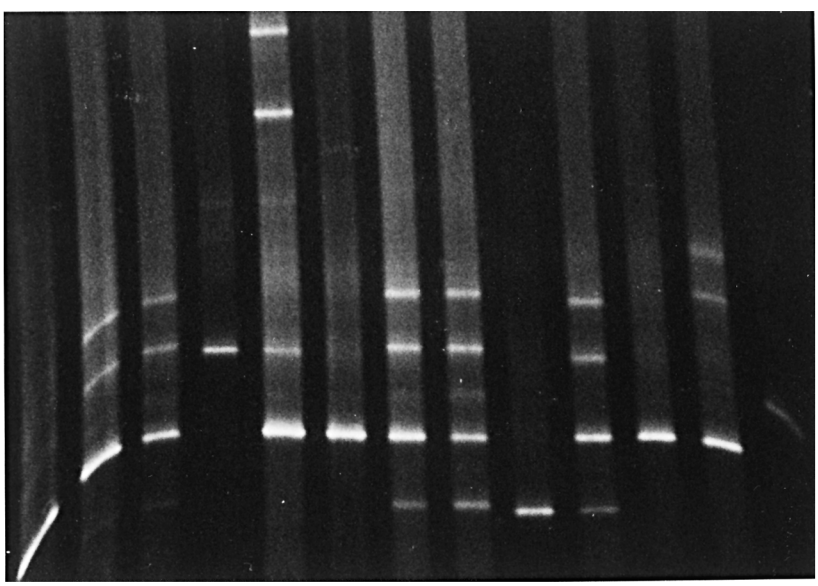

1 2 3 4 5 6 7 8 9 10 11 12 13

16192 16104+16223 16093 16131 16111

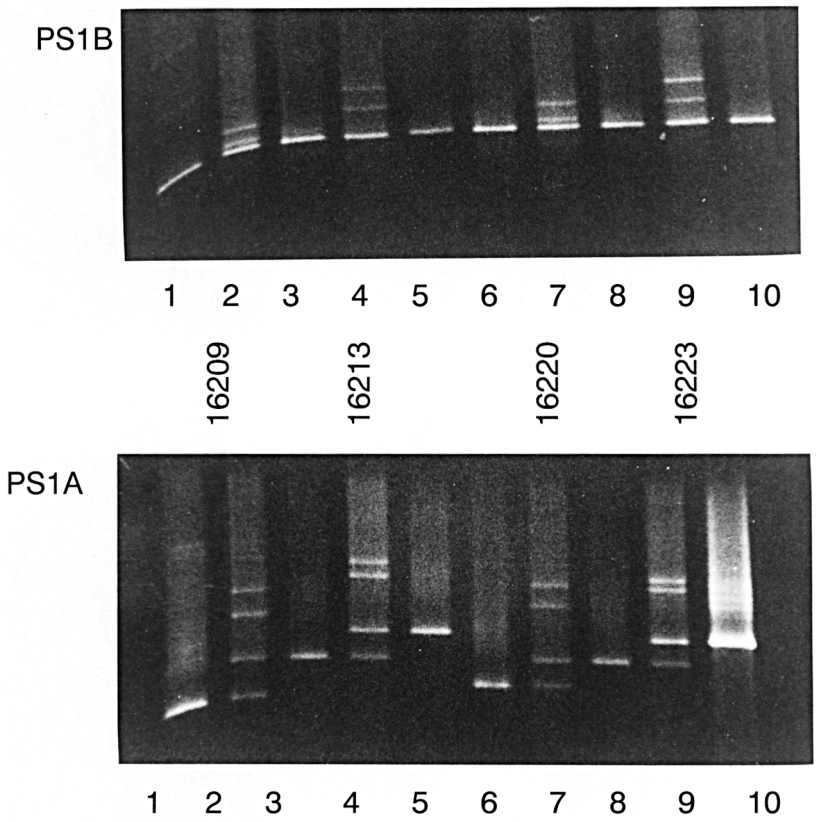

FIG. 5—*This figure depicts the influence of melting domains on separations obtained for both the PS1A and PS1B fragments. Both figures display the same four comparisons, each differing by a single base pair at the indicated positions. The overall sequence composition of PS1A and PS1B is identical, the difference being placement of the GC-clamp and the resulting effect on the melting profile (Fig. 2) of the fragment. Each of the polymorphic differences are located in the intermediate domain of PS1B (Fig. 2). All homoduplexes that remained unresolved with the PS1B fragment, were resolved with the PS1A fragment. Lane assignments for both panels of Fig. 5 are: Lane 1, E44; Lane 2, E44/CRS; Lane 3, CRS; Lane 4, E73/CRS; Lane 5, E73; Lane 6, N3; Lane 7, N3/CRS; Lane 8, CRS; Lane 9, E100/CRS; Lane 10, E100.*

3′ end of the PS1 fragments and included polymorphisms at positions 16184, 16209, 16213, 16220, and 16223. In every case, the homoduplexes that were not resolved with the PS1B fragment were resolved with PS1A (Fig. 5). Analysis of the melt maps and mobility transition gels for the two fragments reveals that all positions were located within the intermediate domain of PS1B and the lowest melting domain for PS1A. Dissociation of the lower melting domain ($T_m \approx 70°C$) in PS1B retards migration such that the position at which the intermediate domain ($T_m \approx 72°C$) would denature is not attained. In contrast, with the PS1A fragment all homoduplexes migrate to the same position in the gel before denaturation occurs. Failure to separate sequences containing polymorphisms in regions other than the lowest melting domain of a sequence has previously been well documented (37,38). However, it is important to emphasize that the heteroduplexes were resolved from the homoduplexes in each case. Those homoduplexes existing within the overlapping region between the primer sets which remained unresolved using the PS1B fragment were also consistently unresolved with the PS2 fragment (we were eventually successful in resolving the individual homoduplexes differing at position 16213 after a 48 h run in a 40–70% gradient using the PS2 fragment). Although more subtle than the clearly defined domains in PS1B, the PS2 melt map and mobility transition curve reveal a slightly higher stability at the 5′ end (again reflecting the higher stability of the middle part of HV1 region) relative to the 3′ end. In this study, the only homoduplexes that remained unresolved under all conditions were those differing by conservative transversions at positions 16239 and 16318. Higuchi et al. (48), calculated the stability of sequences differing by transversions and concluded that the mean stacking temperatures for the homoduplexes in the d(TCA)●d(TGA)>d(TGA)●d(TCA) and d(AAG)●d(CTT)>d(ATG)●d(CAT) configurations would be the same, hence resolution of the homoduplexes at these positions may not be achievable

FIG. 4—*Parallel denaturing gradient gels (37.5–47.5% denaturant) of PCR products amplified with the PS1A primer set. As in Fig. 3 each mixed sample pair is flanked by the individual samples in the adjacent lanes. Figure 4A shows the separations obtained for polymorphisms in five different nearest neighboring environments including two transversions (16037 and 16153). Polymorphic positions are indicated and listed in Table 2. Samples B12 (Lane 3) and M7 (Lane 7) of Fig. 4B are heteroplasmic. Lane 5 of Fig. 4B depicts a comparison of samples differing by two polymorphisms at positions 16104 (C/T) and 16223 (C/T): Lane assignments are as follows:* Figure 4A: *Lane 1, E53; Lane 2, E53/E99; Lane 3, E99; Lane 4, B11; Lane 5, B11/B10; Lane 6, B10; Lane 7, B15; Lane 8, B15/CRS; Lane 9, CRS; Lane 10, E117/CRS; Lane 11, E117; Lane 12, E114; Lane 13, E114/E111; Lane 14, E111.* Figure 4B: *Lane 1, CRS; Lane 2, B12/CRS; Lane 3, B12; Lane 4, B17; Lane 5, B17/CRS; Lane 6, CRS; Lane 7, M7/CRS; Lane 8, M7; Lane 9, B18; Lane 10, B18/CRS; Lane 11, CRS; Lane 12, E47/CRS; Lane 13, E47.*

(the homoduplexes for all other transversions listed in Table 2 were resolved which is also consistent with Higuchi et al.'s findings).

Separation of the homoduplexes is especially important for identifying positions of heteroplasmy. Our current procedure requires that each band be re-amplified after excision from the gel. Re-amplification of sequences containing a mismatch produces a mixed sequence at the position of the mismatch (as shown in Fig. 7), as does re-amplification of a band containing two unresolved homoduplexes. Ideally, unambiguous identification of a heteroplasmic position requires discrimination between bands. Sequencing both strands from one of the heteroduplex bands directly after elution from the gel would greatly simplify the procedure permitting identification of the heteroplasmic position based upon the difference in sequence between the two strands. Furthermore, it would be better to retest the original sample in isolation rather than to excise and re-amplify a suspected heteroplasmic band from a comparison gel due to the potential for cross-contamination.

Analysis of Multiple Base Pair Differences on Parallel Denaturing Gradient Gels

Multiple mismatches, which may be found in comparisons of unrelated individuals, or from contamination, would be expected to further destabilize the helix resulting in an increased resolution between homo- and heteroduplexes. Sequences differing by two, three, four, and five base pairs are shown in Fig. 6 (see also Fig. 4). Consistent with their lower stability, heteroduplexes containing greater than one mismatch denature earlier in the gradient relative to those containing only a single mismatch and are well resolved from their respective homoduplexes. The large destabilization imposed by multiple mismatches results in the heteroduplexes denaturing very shortly after entering the gel in 10% gradients, often with no resolution between the individual heteroduplex sequences. The 20% gradient of Fig. 6 allows for resolution of all bands and would be preferred over a 10% gradient when no prior knowledge as to the number of polymorphic differences exist between two sequences. The broadened bands seen with the heteroduplexes in comparisons of sequences differing by four and five polymorphisms are most likely the consequence of the bands not fully focusing within the time frame of the gel run. However, we occasionally see a more severe form of "band broadening" with heteroduplexes differing by multiple polymorphisms. Imposing a second, co-linear acrylamide gradient in the gel was recently reported (49,50) to be effective in resolving band broadening which in some cases is severe enough to spread the band out over a distance of about a centimeter on the gel.

Analysis of Heteroplasmy

PCR product from DNA extracted from bone samples of Georgij and Nicholas Romanov, both of whom were previously shown to be heteroplasmic at position 16169 (C+T) by sequencing (51,52) were analyzed by DGGE (Fig. 7). Additional heteroplasmic samples are shown in Lane 4 of Fig. 3B (16309 A+G), and Lane 3 (16192 T+C) and Lane 7 (16093 T+C) of Fig. 4B. For both the 16309 and 16093 heteroplasmic samples, the individual haplotypes

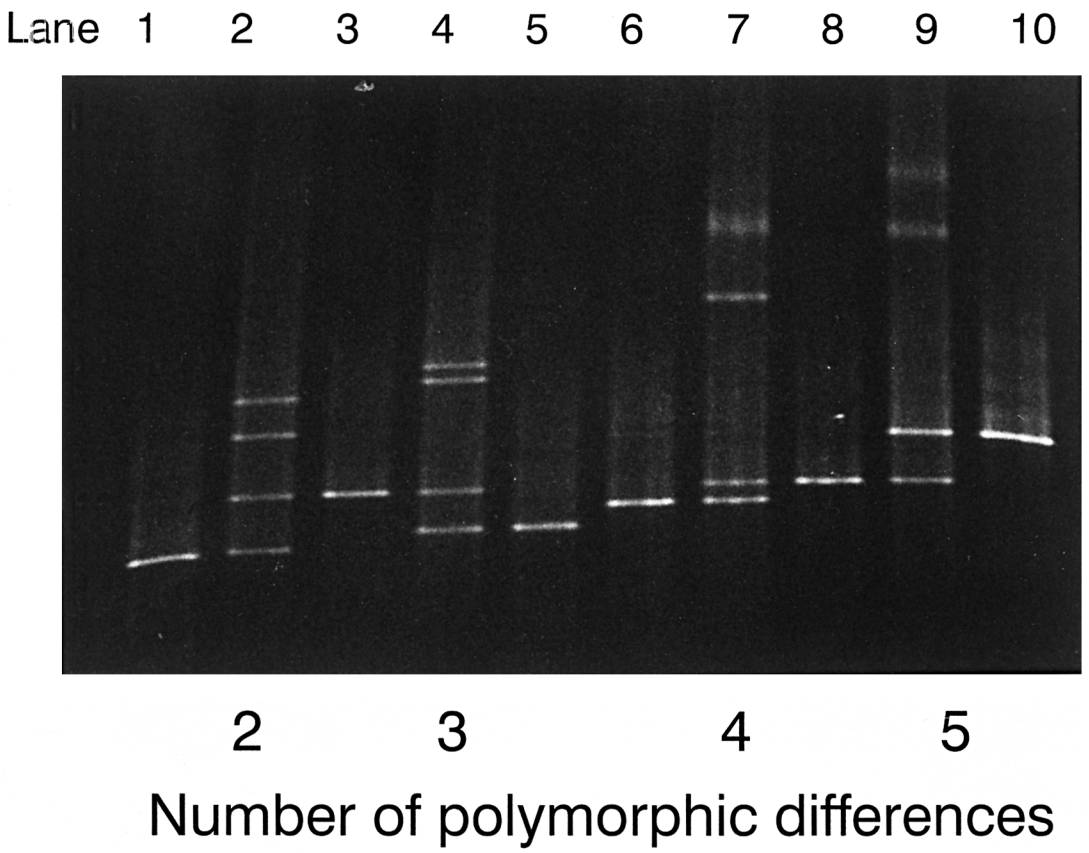

FIG. 6—*PCR products (PS2 fragment) differing by the indicated number of polymorphisms on a 35–55% denaturant gradient gel (8% acrylamide). Lane assignments are as follows: Lane 1, B19; Lane 2, B19/CRS; Lane 3, CRS; Lane 4, B20/CRS; Lane 5, B20; Lane 6, B21; Lane 7, B21/CRS; Lane 8, CRS; Lane 9, B22/CRS; Lane 10, B22. Polymorphic differences are: B11/CRS; 16224 (T/C), 16311 (T/C); B20/CRS, 16193 (C/T), 16219 (A/G), 16362 (T/C); B21/CRS; 16172 (T/C), 16223 (C/T), 16311 (T/C), 16319 (G/A); B22/CRS; 16172 (T/C), 16192 (C/T), 16256 (C/T), 16270 (C/T), 16291 (C/T).*

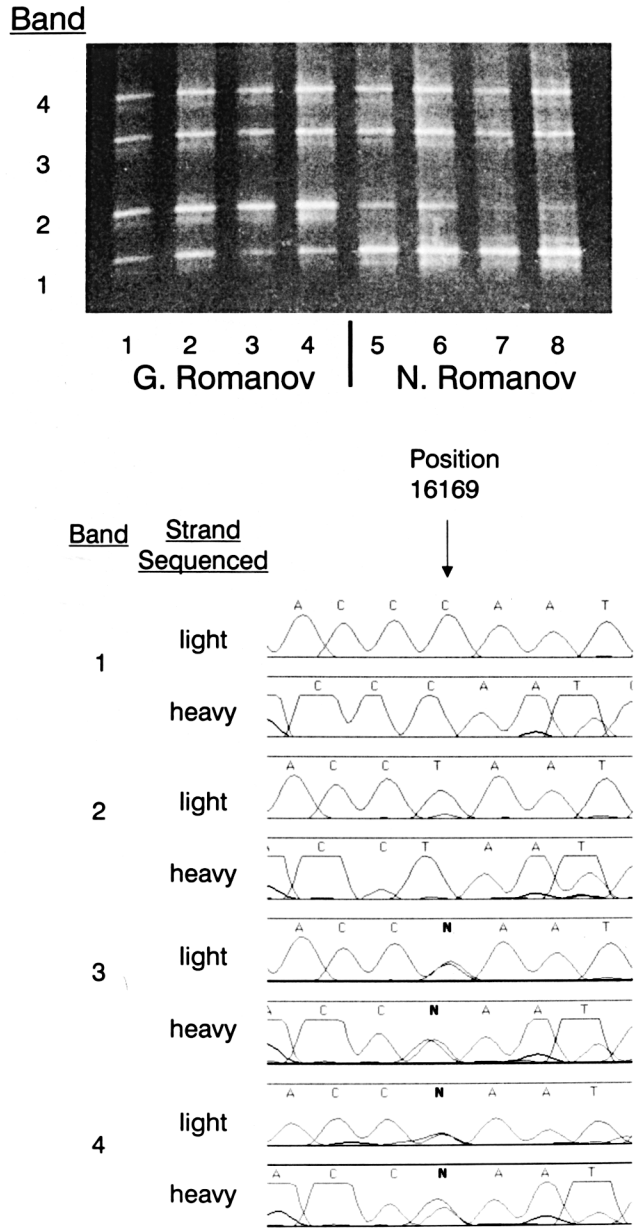

FIG. 7—*Analysis of PCR product (fragment PS1C) amplified from bone extracts of Georgij (lanes 1–4) and Nicholas Romanov (lanes 5–8). Previous studies based on sequence analysis revealed heteroplasmy at position 16169 (C+T) (51,52). Four separate lanes were run for each sample and percent of each haplotype per lane calculated from band intensities and then averaged for all four lanes per individual. The d(CTA)●d(TAG) and d(CCA)●d(TGG) haplotypes were found to be present at 68% (+/−7.8) and 32% (+/−6.8), respectively, in Georgij Romanov and 29% (+/−4.6) and 71% (+/−4.6), respectively, in Nicholas Romanov. This is in excellent agreement with those values obtained by analysis of peak heights from sequencing (62% and 38% in Georgij Romanov and 28% and 72% in Nicholas Romanov) (Ivanov et al. 1996). Each individual band in lanes four and six were excised, re-amplified, and sequenced with identical results. The sequences obtained from each band (both mtDNA heavy and light strands) from lane four are shown. Band one and two constitute the homoduplexes, and band three and four the heteroduplexes. The stability of single base polymorphisms and mismatches in the d(CXA)●d(TYG) sequence environment was analyzed by Ke and Wartell (30), with d(CCA)●d(TGG) found to be more stable then the d(CTA)●d(TAG), consistent with the results obtained here. Assuming a consistent ordering of stability, band 3 is predicted to arise from amplification of a template having the d(CTA)●d(TGG) mismatch and band 4 the d(CCA)●d(TAG) mismatch.*

are present at similar concentrations and both homoduplex bands are easily identifiable. Figure 8 displays a mixture experiment designed to mimic heteroplasmy in which two sequences differing by a single base pair (position 16126, T+C) were mixed at the indicated ratios prior to amplification. Sequences present at concentrations as low as 1:100 may be identified, however, dilution by mass action with the complementary strands of the major haplotype precludes detection of an independent homoduplex band for the minor haplotype. Similarly, the homoduplex band for the 16192 (T) sample is present at much lower concentration than that for the 16192 (C) haplotype (Lane 5, Fig. 4B). Previous sensitivity estimates for detecting heteroplasmy from sequencing alone is 10–20% (53). In the course of this study, heteroplasmy was found twice in unrelated individuals at positions 16093 (T+C), 16172 (T+C), and 16309 (G+A), and once at the other positions indicated in Table 2. Only one was a transversion (position 16318, A+T). In each case, except for the Romanov's samples and sample R1 (sample consumed), at least two separate extractions, amplifications, and DGGE analyses of the sample were performed.

Discussion

The DGGE assay described constitutes a conceptually simple, accurate, and inexpensive comparative test for determining whether two sequences match in the HV1 region of the mtDNA D-loop. A second benefit is the unambiguous identification of co-amplifying contaminating, or heteroplasmic sequences in the independent sample lanes. This later capacity cannot be overstated due to the increased emphasis on contamination of evidentiary material in the legal arena and in mitochondrial analysis of ancient remains. Although reagent blanks and negatives are effective in identifying contamination arising systematically, they are not effective at identifying samples which are contaminated in situ, or that which may occur sporadically during sample processing. Although not absolutely required, verifying the homogeneity of the actual sample tested is arguably the more germane control. Sequence data obtained from mixed samples is difficult to interpret because more than one peak is present at the different polymorphic positions between the two samples. Since unrelated individuals differ by an average of 4.59 nucleotides (Caucasians) (41) in the HV1 region, and excluding length-based heteroplasmy in the polycytosine "C-stretch" region, heteroplasmy is rarely seen at more than one position (for exceptions, see Refs 53–55), the number of polymorphisms existing between two sequences may aid in discriminating between contamination or heteroplasmy.

Sequence-based heteroplasmy in the HV1 region is important to identify due to the potential increase in the discriminatory potential (as evidenced in the Romanov case), and to eliminate any potential confusion in determining the sequence for the sample. Previous researchers have found an increase in the occurrence of heteroplasmy in the mtDNA D-loop relative to coding regions of the mtDNA genome (56), and it may be a more common phenomena than has previously been thought (57,58). Typically, sequence-based heteroplasmy is seen as a single mixed-base position in an otherwise clean sequence. However, the call can be missed due to complications imposed by the difference in concentrations between the two haplotypes (53), or by the differential incorporation of nucleotides by the polymerases used in cycle sequencing (59).

A second type of heteroplasmy more commonly encountered in casework is length-based heteroplasmy formed by nucleotide insertions in the polycytosine "C-stretch" region (bp 16184–16193)

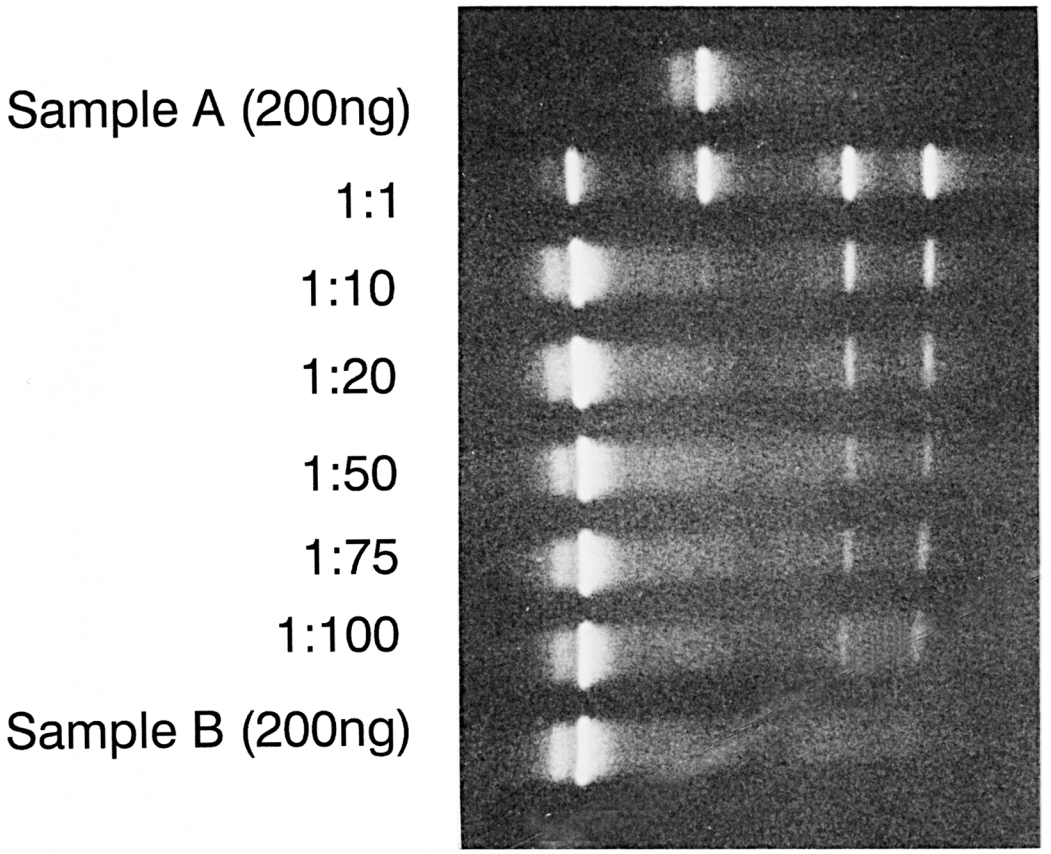

FIG. 8—*This Fig. 8 depicts a mixture experiment designed to mimic mtDNA heteroplasmy. Two PCR products differing by a single base pair (T+C transition at position 16126) were quantitated by ultraviolet light, mixed at the indicated ratios, and re-amplified prior to DGGE analysis. Sequences present at ratios as low as 1:100 may be identified. Primer set used was PS1B.*

(60–63). Sequence analysis results in good data for all nucleotides proximal, in relation to the sequencing primer, and poor distal to the region, regardless of which strand is sequenced. Due to the difficulties in obtaining reliable sequence data for the region, the number of insertions in HV1 is usually not called in casework. Analysis of samples known to display length-based heteroplasmy results in a characteristically complex banding pattern on denaturing gradient gels (data not shown) due to the large number of heteroduplex combinations which may be formed during the PCR reaction and dilution by mass action of those sequences present at lower concentrations. Absolute verification for the resolution of all six known potential length variants (61,62) in this region by DGGE would require testing the isolated, individual sequences (which were unavailable). In general, we have found it impractical to analyze individual species from samples containing more than three sequences.

Including the heteroplasmic samples identified in this study, we have analyzed 55 pairs of sequences differing by a single base pair at separate sites within the 342 base pair HV1 region. We have not found any that we were unable to discriminate between. Using the related technique of temperature gradient gel electrophoresis, Ke and Wartell (30,64,65) have measured the relative stability differences of single base polymorphisms, single and tandem mismatches, and single base bulges in a 373 base pair sequence within four different defined nearest neighbor environments. The difference in stability of a single polymorphism between two otherwise identical sequences ranged between 0–1.7°C, with G●C and C●G base pairs more stable than A●T and T●A base pairs. Single base pair mismatches lower the stability with respect to the fully base-paired homoduplexes by 1-5°C, with both composition and sequence context of the mismatch affecting stability. Single-base bulges, which may be expected to arise from hybridization of different length variants in the "C-stretch" region, lower stability by 2-3.6°C. The sharp focusing of bands on the gels, resulting from the progressive denaturation of sequences at their T_m, allow a separation of 1–2 mm to be obtained. In this study, a 10% difference in gradient concentration, equivalent to 3.1°C (26), was imposed over a 22 cm gel or 0.14°C/cm. Considering the temperature stability differences found by Ke and Wartell, and the stringency of the gradient employed, it is difficult to envision a sequence containing a mismatch within the lowest melting domain in any of the fragments analyzed not being resolved from its respective homoduplex. However, anomalous migration of sequences in DGGE has been previously reported, usually associated with non-β-form DNA structures (66–68) or band broadening associated with fragments containing a low domain flanked by two higher domains (69). While we have seen no evidence of non-β-form structures in the PCR products analyzed, we do see band broadening in the heteroduplex bands differing by multiple polymorphisms which is occasionally severe, but in no way precludes discrimination between samples.

In conclusion, DGGE can improve the overall throughput of lab-

oratories involved in mtDNA testing by identifying matching sequences prior to sequencing and provide a more definitive control for the identification of heteroplasmy or co-amplifying contaminating sequences than is presently available.

Acknowledgments

We would like to thank the AFDIL staff for extraction and sequencing of many of the samples used in this study. Special thanks to the Armed Forces Institute of Pathology, the Office of the Armed Forces Medical Examiner, and the American Registry of Pathology for their support.

References

1. Stoneking M, Hedgecock D, Higuchi RG, Vigilant L, Erlich HA. Population variation of human mtDNA control region sequences detected by enzymatic amplification and sequence-specific oligonucleotide probes. Am J Hum Genet 1991;48:370–82.
2. Sullivan KM, Hopgood R, Gill P. Identification of human remains by amplification and automated sequencing of mitochondrial DNA. Int J Leg Med 1992;105:83–6.
3. Ginther C, Issel-Tarver L, King MC. Identifying individuals by sequencing mitochondrial DNA from teeth. Nat Genet 1992;2:135–38.
4. Wilson MR, DiZinno JA, Polanskey D, Replogle J, Budowle B. Validation of mitochondrial DNA sequencing for forensic casework analysis. Int J Leg Med 1995;108:68–74.
5. Holland MM, Fisher DL, Roby RK, Ruderman J, Bryson C, Weedn VW. Mitochondrial DNA sequence analysis of human remains. Crime Lab Digest 1995;22:109–15.
6. Lutz S, Weisser H-J, Heizmann J, Pollak S. mtDNA as a tool for identification of human remains identification using mtDNA. Int J Leg Med 1996;109:205–9.
7. Avise JC, Lansman RA. Polymorphism of mitochondrial DNA in populations of higher animals. In: Nei M, Koehn RK, editors. Evolution of genes and proteins. Sunderland, Mass: Sinauer Associates 1983;147–90.
8. Avise JC, Saunders NC. Mitochondrial DNA and the evolutionary genetics of higher animals. Genetics 1984;108:237–55.
9. Cann RL, Stoneking M, Wilson AC. Mitochondrial DNA and human evolution. Nature 1987;325:31–6.
10. Chakraborty B, Weiss KM. Genetic variation of the mitochondrial DNA genome in American indians is at mutation-drift equilibrium. Am J Phys Anthrop 1991;86:497–506.
11. Aquadro CF, Greenberg, BD. Human mitochondrial DNA variation and evolution: analysis of nucleotide sequences from seven individuals. Genetics 1983;103:287–312.
12. Greenberg BD, Newbold JE, Sugino A. Intraspecific nucleotide sequence variability surrounding the origin of replication in human mitochondrial DNA. Gene 1983;21:33–49.
13. Cann RL, Brown WM, Wilson AC. Polymorphic sites and the mechanism of evolution in human mitochondrial DNA. Genetics 1984;106:479–99.
14. Vigilant L, Pennington R, Harpending H, Kocher TD, Wilson AC. Mitochondrial DNA sequence in single hairs from a single southern African population. Proc Natl Acad Sci USA 1989;86:9350–4.
15. Horai S, Hayasaki K. Intraspecific nucleotide sequence differences in the major noncoding region of human mitochondrial DNA. Am J Hum Genet 1990;46:828–42.
16. Ward RH, Frazier BL, Dew-Jager K, Paabo S. Extensive mitochondrial diversity within a single Amerindian tribe. Proc Natl Acad Sci USA 1991;88:8720–24.
17. Giles RE, Blanc H, Cann HM, Wallace DC. Maternal inheritance of human mitochondrial DNA. Proc Natl Acad Sci USA 1980;77:6715–19.
18. Orrego C, King MC. Determination of familial relationships. In: Innis MA, Gelfind DH, Sninsky JJ, White JJ, editors. PCR protocols: a guide to methods and applications. London: Academic Press Inc, 1990; 416–26.
19. Sullivan KM, Hopgood R, Lang B, Gill P. Automated amplification and sequencing of human mitochondrial DNA. Electrophoresis 1991; 12:17–21.
20. Hopgood R, Sullivan KM, Gill P. Strategies for automated sequencing of human mitochondrial DNA directly from PCR products. Biotechniques 1992;13:60–8.
21. Wilson MR, Stoneking M, Holland MM, DiZanno JA, Budowle B. Guidelines for the use of mitochondrial DNA sequencing in forensic science. Crime Lab Digest 1993;20:68–77.
22. Fischer SG, Lerman LS. DNA fragments differing by single base-pair substitutions are separated in denaturing gradient gels: correspondence with melting theory. Proc Natl Acad Sci USA 1983;80:1579–83.
23. Lerman LS, Fischer SG, Hurley I, Silverstein K, Lumelsky N. Sequence-determined DNA separations. Ann Rev Biophys Bioeng 1984;13: 399–423.
24. Myers RM, Lumelsky N, Lerman LS, Maniatis T. Detection of single base substitutions in total genomic DNA. Nature (London) 1985;313: 495–8.
25. Myers RM, Maniatis T, Lerman LS. Detection and localization of single base changes by denaturing gradient gel electrophoresis. Methods in Enzymology 1987;155:501–27.
26. Lerman LS, Silverstein K. Computational simulation of DNA melting and its application to denaturing gradient gel electrophoresis. Methods in Enzymology 1987;155:482–501.
27. Abrams ES, Stanton Jr VP. Use of denaturing gradient gel electrophoresis to study conformational transitions in nucleic acids. Methods in Enzymology 1992;212:71–104.
28. Fodde R, Losekoot M. Mutation detection by denaturing gradient gel electrophoresis (DGGE). Hum Mut 1994;3:83–94.
29. Rossenbaum V, Reissner D. Temperature-gradient gel electrophoresis. Thermodynamic analysis of nucleic acids and proteins in purified form in cellular extracts. Biophys Chem 1987;26:235–46.
30. Wartell RM, Hosseini SH, Moran CP. Detecting base pair substitutions in DNA fragments by temperature-gradient gel electrophoresis. Nuc Acids Res 1990;18:2699–705.
31. Ke S-H, Wartell RM. Influence of nearest neighbor sequence on the stability of base pair mismatches in long DNA: determination by temperature-gradient gel electrophoresis. Nuc Acids Res 1993;21:5137–43.
32. Borresen A, Hovig E, Smith-Sorenson B, Malkin D, Lystad S, Andersen TI, et al. Constant denaturant gel electrophoresis as a rapid screening technique for p53 mutations. Proc Natl Acad Sci USA 1991;88:8405–9.
33. Hovig E, Smith-Sorenson B, Brogger A, Borresen A. Constant denaturant gel electrophoresis, a modification of denaturing gradient gel electrophoresis, in mutation detection. Mut Res 1991;262:63–71.
34. Smith-Sorenson B, Hovig E, Anderson B, Borresen A. Screening for mutations in human HPRT cDNA using the polymerase chain reaction (PCR) in combination with constant denaturant gel electrophoresis (CDGE). Mut Res 1992;269:41–53.
35. Khrapko K, Hanekamp JS, Thilly WG, Belenkil A, Foret F, Karger BL. Constant denaturant capillary electrophoresis (CDCE): a high resolution approach to mutational analysis. Nuc Acids Res 1994;22:364–9.
36. Gelfi C, Cremonesi L, Ferrari M, Righetti PG. Temperature-programmed capillary electrophoresis for detection of DNA point mutations. Biotechniques 1996;21:926–32.
37. Lerman LS, Silverstein K, Grinfeld E. Searching for gene defects by denaturing gradient gel electrophoresis. Cold Spring Harbor Symposium on Quantitative Biology 1986;LI:285–97.
38. Abrams ES, Murdaugh SA, Lerman LS. Comprehensive detection of single base changes in human genomic DNA using denaturing gradient gel electrophoresis and a GC clamp. Genomics 1990;7:463–75.
39. Paabo S. Ancient DNA: extraction, characterization, molecular cloning, and enzymatic amplification. Proc Natl Acad Sci USA 1989;86: 1939–43.
40. Lindahl T. Instability and decay of the primary structure of DNA. Nature 1993;362:709–15.
41. Piercy R, Sullivan KM, Benson N, Gill P. The application of mitochondrial DNA typing to the study of white caucasian identification. Int J Leg Med 1993;106:85–90.
42. Walsh PS, Metzger DA, Higuchi R. Chelex 100 as a medium for simple extraction of DNA for PCR-based typing from forensic material. Biotechniques 1991;10:506–13.
43. Anderson S, Bankier AT, Barrell BG, deBruijn MHL, Coulson AR, Drouin J, et al. Sequence and organization of the human mitochondrial genome. Nature 1981;290:457–65.
44. Myers RM, Fischer SG, Lerman LS, Maniatis T. Nearly all single base substitutions in DNA fragments joined by a GC-clamp can be detected by denaturing gradient gel electrophoresis. Nuc Acids Res 1985;13: 3131–45.
45. Myers RM, Fischer SG, Maniatis T, Lerman LS. Modification of the melting properties of duplex DNA by attachment of a GC-rich DNA sequence as determined by denaturing gradient gel electrophoresis. Nuc Acids Res 1985;13:3111–29.
46. Sheffield VC, Cox DR, Lerman LS, Myers RM. Attachment of a 40-

base-pair G+C-rich sequence (GC-clamp) to genomic DNA fragments by the polymerase chain reaction results in improved detection of single-base changes. Proc Natl Acad Sci USA 1989;86:232–6.
47. Steger G. Thermal denaturation of double-stranded nucleic acids: prediction of temperatures critical for gradient gel electrophoresis and polymerase chain reaction. Nuc Acids Res 1994;22:2760–8.
48. Higuchi M, Antonarakis SE, Kasch L, Oldenburg J, Economou-Peterson E, Olek K, et al. Molecular characterization of mild-to-moderate hemophilia A: detection of the mutation in 25 of 29 patients by denaturing gradient gel electrophoresis. Proc Natl Acad Sci USA 1991; 88:8307–11.
49. Cremonesi L, Firpo MS, Ferrari M, Rigehetti PG, Gelfi C. Double-gradient DGGE for optimized detection of DNA point mutations. Biotechniques 1997;22:326–30.
50. Gelfi C, Righetti SC, Zunino F, Della Torre G, Pierotti MA, Righetti PG. Detection of p53 point mutations by double-gradient denaturing gradient gel electrophoresis. Electrophoresis 1997;18:2921–7.
51. Gill P, Ivanov PL, Kimpton C, Piercy R, Benson N, Tully G, et al. Identification of the remains of the Romanov family by DNA analysis. Nature Genet 1994;6:130–5.
52. Ivanov PL, Wadhams MJ, Roby RK, Holland MM, Weedn VW, Parsons TJ. Mitochondrial DNA sequence heteroplasmy in the Grand Duke of Russia Georgij Romanov establishes the authenticity of the remains of Czar Nicholas II. Nature Genet 1996;12:417–22.
53. Bendall KE, Macaulay VA, Baker JR, Sykes BC. Heteroplasmic point mutations in the human mtDNA control region. Am J Hum Genet 1996;59:1276–87.
54. Comas D, Paabo S, Bertranpetit J. Heteroplasmy in the control region of human mitochondrial DNA. Genome Res 1995;5:89–90.
55. Howell N, Kubacka I, Mackey DA. How rapidly does the human mitochondrial genome evolve? Am J Hum Genet 1996;59:501–9.
56. Jazin EE, Cavelier L, Eriksson I, Oreland L, Gyllensten U. Human brain contains high levels of heteroplasmy in the noncoding regions of mitochondrial DNA. Proc Natl Acad Sci USA 1996;93:12382–7.
57. Monnat RJ, Loeb LA. Nucleotide sequence preservation of human mitochondrial DNA. Proc Natl Acad Sci USA 1985;82:2895–9.
58. Monnat RJ, Maxwell CL, Loeb LA. Nucleotide sequence preservation of human leukemic mitochondrial DNA. Cancer Res 1985;45:1809–985.
59. Parker LT, Zakeri H, Deng Q, Spurgeon S, Kwok P-Y, Nickerson DA. AmpliTaq DNA polymerase, FS Dye-Terminator sequencing: analysis of peak height patterns. Biotechniques 1996;21:694–9.
60. Hauswirth WW, Clayton DA. Length heteroplasmy of a conserved displacement-loop sequence in human mitochondrial DNA. Nuc Acids Res 1985;13:8093–104.
61. Bendall KE, Sykes BC. Length heteroplasmy in the first hypervariable segment of the human mtDNA control region. Am J Hum Genet 1995;57:248–56.
62. Marchington DR, Poulton J, Sellar A, Holt IJ. Do sequence variants in the major non-coding region of the mitochondrial genome influence mitochondrial mutations associated with disease? Hum Mol Gen 1996;5:473–9.
63. Marchington DR, Hartshorne GM, Barlow D, Poulton J. Homopolymeric tract heteroplasmy in mtDNA from tissues and single oocytes: support for a genetic bottleneck. Am J Hum Genet 1997;60:408–16.
64. Ke S-H, Wartell RM. Influence of neighboring base pairs on the stability of single base bulges and base pairs in a DNA fragment. Biochemistry 1995;34:4593–600.
65. Ke S-H, Wartell RM. The thermal stability of DNA fragments with tandem mismatches at a d(CXYG)-d(CY′X′G) site. Nuc Acids Res 1996;24:707– 12.
66. McCampbell CR, Wartell RM, Plaskon RR. Inverted repeat sequences can influence melting transitions of linear DNAs. Biopolymers 1989;28: 1745–58.
67. Gray M, Charpentier A, Walsh K, Wu P, Bender W. Mapping point mutations in the drosophila *rosy* locus using denaturing gradient gel electrophoresis. Genetics 1991;127:139–49.
68. Weber CK, Shaffer DJ, Sidman CL. Unexpected behavior of $H2K^b$ mutant DNAs in denaturing gradient gel electrophoresis. Nuc Acids Res 1991;19:3331–5.
69. Abrams ES, Murdaugh SA, Lerman LS. Intramolecular DNA melting between stable helical segments: melting theory and metastable states. Nuc Acids Res 1995;23:2775–83.

Address additional information and reprint requests:
Robert Steighner, Ph.D.
Fairfax Identity Laboratory
Genetics and IVF Institute
3025 Hamaker Court, Suit 203
Fairfax VA, 22031
email: SteighnerB@aol.com